



This is a repository copy of *Heavily tin-doped indium oxide nano-pyramids as high-performance gas sensor*.

White Rose Research Online URL for this paper:
<http://eprints.whiterose.ac.uk/140809/>

Version: Published Version

Article:

Li, Q., Zhang, Y., Wang, Z. et al. (4 more authors) (2018) Heavily tin-doped indium oxide nano-pyramids as high-performance gas sensor. *AIP Advances*, 8 (11). 115316. ISSN 2158-3226

<https://doi.org/10.1063/1.5048622>

Reuse

This article is distributed under the terms of the Creative Commons Attribution (CC BY) licence. This licence allows you to distribute, remix, tweak, and build upon the work, even commercially, as long as you credit the authors for the original work. More information and the full terms of the licence here:
<https://creativecommons.org/licenses/>

Takedown

If you consider content in White Rose Research Online to be in breach of UK law, please notify us by emailing eprints@whiterose.ac.uk including the URL of the record and the reason for the withdrawal request.



eprints@whiterose.ac.uk
<https://eprints.whiterose.ac.uk/>

Heavily tin-doped indium oxide nano-pyramids as high-performance gas sensor

Cite as: AIP Advances **8**, 115316 (2018); <https://doi.org/10.1063/1.5048622>

Submitted: 16 July 2018 . Accepted: 07 November 2018 . Published Online: 15 November 2018

Qiang Li , Yuantao Zhang, Zuming Wang, Yufeng Li, Wen Ding, Tao Wang, and Feng Yun



View Online



Export Citation



CrossMark

ARTICLES YOU MAY BE INTERESTED IN

[Optical investigation of semi-polar \(11-22\) \$Al_xGa_{1-x}N\$ with high Al composition](#)

Applied Physics Letters **110**, 091102 (2017); <https://doi.org/10.1063/1.4977428>

[Stimulated emission from semi-polar \(11-22\) GaN overgrown on sapphire](#)

AIP Advances **7**, 045009 (2017); <https://doi.org/10.1063/1.4981137>

[Influence of lateral growth on the optical properties of GaN nanowires grown by hydride vapor phase epitaxy](#)

Journal of Applied Physics **122**, 205302 (2017); <https://doi.org/10.1063/1.4998485>

Don't let your writing
keep you from getting
published!

AIP | Author Services

Learn more today!



Heavily tin-doped indium oxide nano-pyramids as high-performance gas sensor

Qiang Li,^{1,2,3} Yuantao Zhang,² Zuming Wang,² Yufeng Li,² Wen Ding,² Tao Wang,^{3,a} and Feng Yun^{1,2,a}

¹Key Laboratory of Physical Electronics and Devices for Ministry of Education and Shaanxi Provincial Key Laboratory of Photonics & Information Technology, Xi'an Jiaotong University, Xi'an, Shaanxi 710049, P. R. China

²School of Electronic and Information Engineering, Xi'an Jiaotong University, Xi'an, Shaanxi 710049, P. R. China

³Department of Electronic and Electrical Engineering, University of Sheffield, Mappin Street, Sheffield S1 3JD, United Kingdom

(Received 16 July 2018; accepted 7 November 2018; published online 15 November 2018)

Heavily Sn-doped In₂O₃ nano-pyramids with a Sn percentage of 19.97% by weight have been prepared by sputtering technique. The nano-pyramids with smooth facets and a sharp tip have been achieved by deposition on Sn-metal particles, leading to a diameter of ~100nm. The gas sensors realized from these pyramids are highly sensitive to ethanol gas, and the sensitivity is about 133.99 against 200ppm ethanol at 250°C. Good sensitivity characteristics have been obtained even at a low temperature of down to 50°C. The high response and low working temperature demonstrate the potential application of heavily Sn-doped In₂O₃ nano-pyramids for fabricating gas sensors. © 2018 Author(s). All article content, except where otherwise noted, is licensed under a Creative Commons Attribution (CC BY) license (<http://creativecommons.org/licenses/by/4.0/>). <https://doi.org/10.1063/1.5048622>

Gas sensing has received increasing attention in both industry and academia, one of the key components for intelligent systems, which has become significantly important for widespread applications in the fields of automotive industry, medical instrumentation, indoor air quality supervision, and environmental studies.¹ Recently, the constantly evolving market demands driven by low cost, timely and accurate gas sensors have led to massive researches in developing the advanced sensing materials.² Metal oxide semiconductor materials have been frequently used to detect various flammable/toxic dangerous gases.³ In order to not only improve gas sensing response but also decrease working temperatures, metal doping has been widely employed introducing defects into the crystalline lattice of a matrix.^{4–9} An increase in metal doping level is expected to enhance the generation of oxygen vacancies. Generally speaking, oxygen vacancies play an important role in obtaining the highly sensitive response of a gas sensor.^{10,11} As a consequence, it is an effective way to enhance the response of gas sensors by increasing the concentration of oxygen vacancies in the materials.

The Tin (Sn) -doped In₂O₃ materials (typically labeled as ITO), known for use in transparent conductive films, have been often employed to detect methanol, formaldehyde, ethanol, CO₂, NH₃, NO₂, and etc.^{12–15} In the previous works, various ITO nano/microstructures have been synthesized, for example, nanoparticles,¹⁶ nanowires,¹⁷ nanoflowers,¹⁸ and microtubule.² The fabrication processes of these nano/micro-devices are complicated. Due to a limited maximum sensitivity and high operation temperatures, the ITO-based sensing devices possess a number of critical limitations. Therefore, it is crucial to improve Sn doping levels and then explore how oxygen vacancies affect the sensing behaviors of ITO-based sensors.

In this work, In₂O₃ nano-pyramids have been deposited on Sn-metal particles by a sputtering technique, achieving a high weight percentage of Sn, up to 19.97% (wt%). Compared with the ITO thin film and the nanowire devices reported previously, our heavily Sn-doped In₂O₃ nano-pyramids

^aCorresponding author e-mail: t.wang@sheffield.ac.uk; fyun2010@mail.xjtu.edu.cn.

feature with both a high gas response and a low working temperature. Taking alcohol as an example, the sensitivity of the device is about 133.99 against 200 ppm obtained at 250°C. Moreover, gas sensing characteristics can still be observed at a temperature of as low as 50°C. We explained the mechanism of the high performance gas sensing properties by using the electric field induced by oxygen vacancy.

A Sn film with a thickness of 60 nm was initially prepared on a Si substrate by a thermal evaporation technique (Fig. 1a). This sample was placed in the sputtering chamber for 30 minutes under pressure less than 3×10^{-4} Pa at 500°C. During this holding period, the Sn film changed into Sn-particles (Fig. 1b). Subsequently, an ITO target ($\text{In}_2\text{O}_3:\text{SnO}_2=9:1$, wt%) was used for sputtering for 20 minutes under a radio-frequency (RF) power of 250W, where an oxygen flow rate of 0.2 sccm was adopted. Finally, the sample was cooled naturally and the nano-pyramids were fabricated (Fig. 1c).

Fig. 1d shows a typical scanning electron microscopy (SEM) image of the fabricated products on the Si substrate. The Sn film is evolved into large aggregated particles at a high temperature such as 500°C which is used for the deposition of ITO target. The In_2O_3 nano-pyramids begin to grow based on these Sn-metal particles, and then exhibiting like a peony flower. Fig. 1e is the enlarged SEM image of a single Sn-island with pyramids, and Fig. 1f is the partial enlarged detail on the top of Sn-island. Energy-dispersive X-ray spectroscopy (EDS) measurements have been conducted, confirming that the pyramids on Sn islands exhibit In, Sn, and O with a weight ratio of 54.77: 19.97: 21.97. The depth range of EDS measurement is 100nm-1 μm (Apollo XL-SDD Det). In order to avoid the detecting result from the Sn metal, many different parts of the nano-pyramids were selected to measure (Fig. S1). This ratio is almost the same on different pyramids (see EDS spectra in [supplementary material](#), Figs. S2 and S3). This means that the Sn doping level of In_2O_3 nano-pyramids prepared on the Sn islands, where Sn-metal plays a kind of role as a catalyst, can be up to 19.97%, which is much higher than that of any standard ITO reported so far.

As displayed in Figs. 1e and 1f, well-aligned tetragonal nano-pyramids with smooth facets and a sharp tip have been achieved. It is visible that every pyramid is enclosed by four triangle facets and one square bottom facet. In order to determine the crystal structure of the pyramids, X-ray diffraction (XRD) experiments were conducted. A XRD spectrum was shown in Fig. 2. There are three major diffraction peaks, which are indexed to the (222), (400), and (440) crystal lattice planes of cubic bixbyite In_2O_3 . The square and triangular facets of the pyramid are indexed to the (400) and (222) planes, respectively.¹⁹ The nano-pyramids exhibit a good uniformity in shape and diameter with a typical value of 100 nm.

Subsequently, these Sn-doped In_2O_3 nano-pyramids were used to fabricate gas sensors. For a gas sensor used in measurement, ceramic tubes with heating wires were used as substrates directly (Fig. S4-a). The sensor was connected with an external electronic circuit, which is used to monitor the

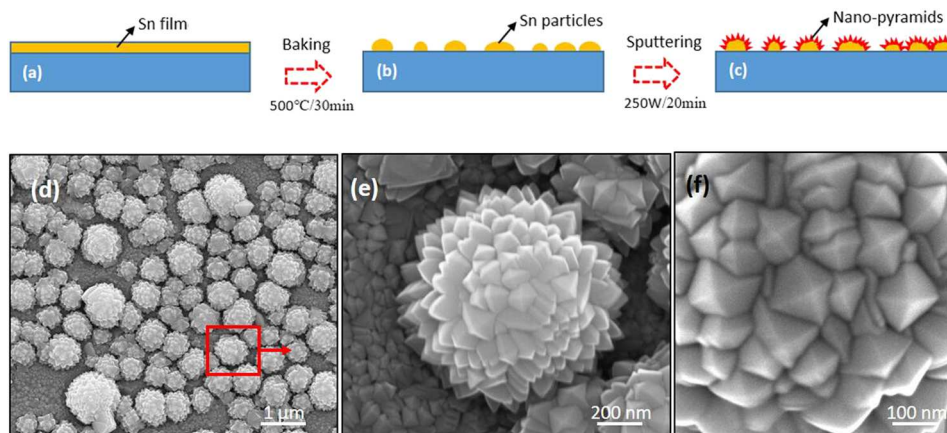


FIG. 1. (a)-(c) The preparation process of nano-pyramids. (d)-(f) The SEM images of Sn-doped In_2O_3 pyramids. (d) the pyramids on Sn islands; (e) a single Sn-island with pyramids; (f) the partial enlarged detail on the top of Sn-island.

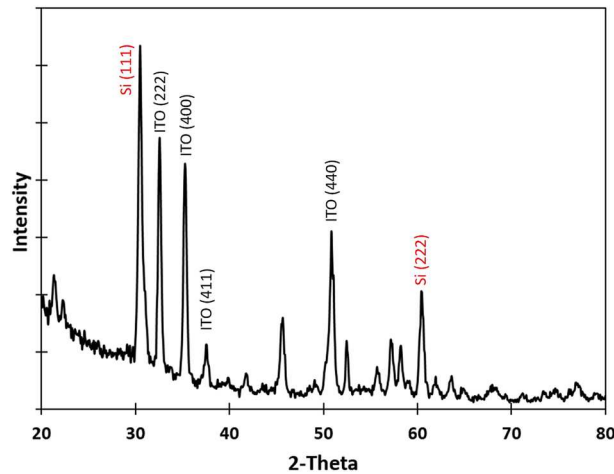


FIG. 2. The XRD patterns for Sn-doped In_2O_3 pyramids on Si substrate.

change in sensor output voltage (Fig. S4-b). The voltage changed after putting the sensor in the gas chamber, which was installed with test gas. The gas-sensing properties of the devices were tested on a WS-30A gas sensor system (Wei-Sheng Electronics Co. Ltd., Zhengzhou, China) under a relative humidity less than 30% RH. In order to eliminate the effect of materials' mass on the devices, the sensitivity (response per mass) was proposed, and defined as $R_{\text{air}}/(m \cdot R_{\text{gas}})$, where R_{air} and R_{gas} are the resistance values measured in the air and reducing-gas ambiances, respectively; and m stands for the mass of the coated sensing materials. The detailed calculation process of sensitivity has been described in the [supplementary material-II](#). The response time t_{res} was defined as the time required for the variation in resistance to reach 90% of the equilibrium value after injection of a test gas, and the recovery time (t_{rec}) was the time necessary for the sensor to 10% of its original resistance in air.

Fig. 3a shows the response and recovery of Sn-doped In_2O_3 nano-pyramids gas sensor upon being exposure to ethanol ambient with 100, 200, 300, 400, and 500 ppm at the working temperature of 250°C. As a comparison, the gas-sensing results on the sample of ITO grown on bare Si substrate under the same conditions were also shown in Fig. 3a. The gas sensing properties of nano-pyramids were characterized in Fig. 3b. The sensor shows a high response to ethanol gas, and all the response time is shorter than 10 s. Under 200 ppm ethanol exposure, the sensitivity is up to about 133.99, which is relatively higher than those of a standard ITO thin film and nanowires.²⁰

Fig. 4 shows the gas response transient curves when the Sn-doped In_2O_3 nano-pyramids sensor is exposed to 400 ppm ethanol under different working temperatures. We know that the sensitivity is higher at higher temperature, while the gas sensitivity at lower temperature directly determines the application area of the devices. The gas sensor based on heavily Sn-doped In_2O_3 pyramids can have a sensitive gas response at temperature of 50°C, which is much lower than the working temperature of 160°C obtained by Sn-doped In_2O_3 nanotube from the newly reported paper.¹⁰ The sensitivity is about 65.59, indicating that this sensor still has a high sensitivity. To the best of our knowledge, this is the lowest working temperature that can detect gas response at 400 ppm. The high response and low working temperature of Sn-doped In_2O_3 nano-pyramids gas sensors support their promising applications in the industry.

The high gas sensing performance of nano-structures is always explained by the adsorption and desorption of oxygen on the surface with large surface-to-volume ratio, but the hypersensitive properties of nano-pyramids at low working temperature are hard to explain well. Fig. 5 shows the gas reaction process of In_2O_3 pyramid on Sn-island. Because the In_2O_3 pyramids were prepared by using Sn metal as catalyst, the In_2O_3 was heavily doped, resulting in more oxygen vacancies. Moreover, the In_2O_3 nano-pyramids have strong field emission effect and the charge inside has the characteristics of gathering towards the tip.¹⁹ The electric potential formed by the electrons inside the Sn-metal is in equilibrium with the potential of the oxygen vacancies in pyramid when there is

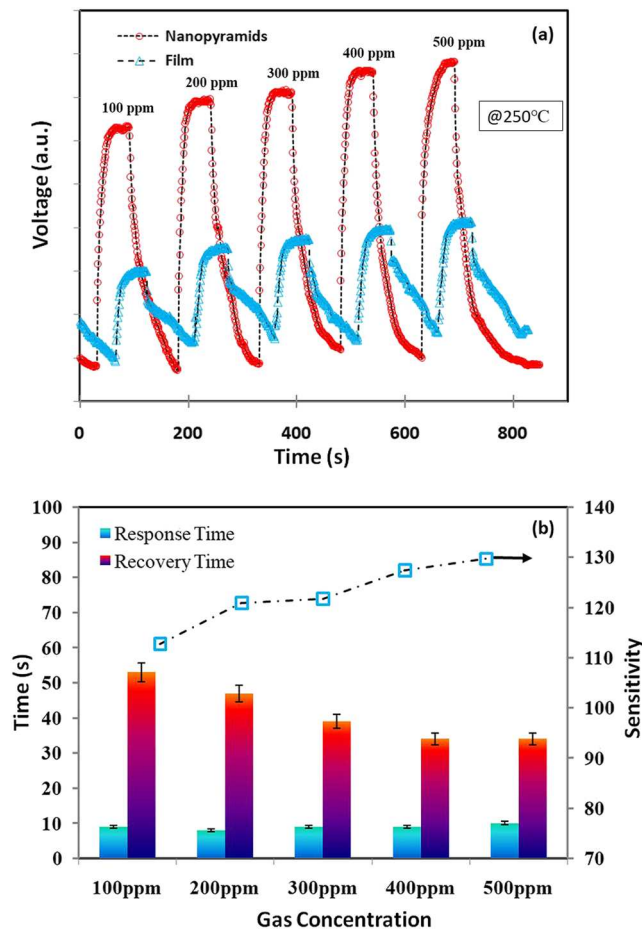


FIG. 3. (a) Real-time dynamic voltage-time (V-T) response curves for 100-500 ppm concentrations of ethanol at 250°C temperature; (b) the response and recovery time, the sensitivity of different gas concentration.

no reaction gas, as shown in Fig. 5a. The surface adsorbed oxygen molecules could turn into oxygen ions via capturing the charges (produced by oxygen vacancies, V_o^-) in the ITO material ($O_2 + 4V_o^- = 2O^{2-}$).²¹ When the reaction gas is exposed, the gas molecules are captured by the oxygen ions (O^{2-})

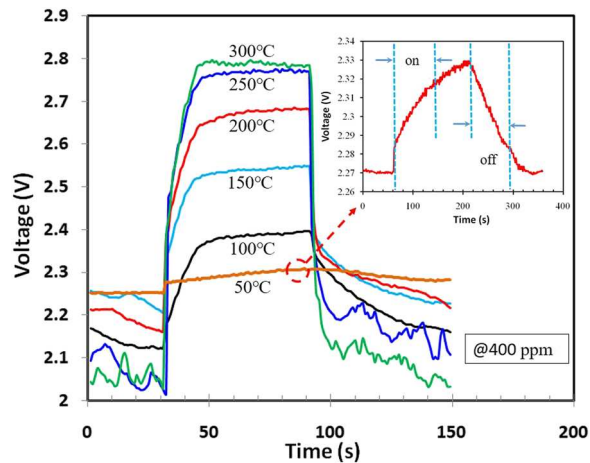


FIG. 4. The response curves for 400 ppm of ethanol at different working temperatures. The insert image is the response curve at the working temperature of 50°C.

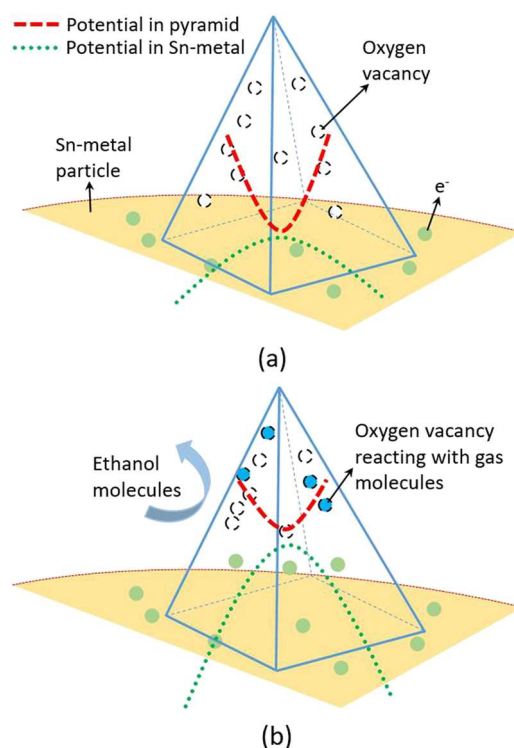


FIG. 5. The schematic illustration for the sensing mechanism of Sn-doped In_2O_3 pyramids in ethanol gas. The potential in pyramid and Sn-metal is in (a) equilibrium state; (b) reaction process.

on the surface of pyramid ($\text{CH}_3\text{CH}_2\text{OH}_{(\text{gas})} + \text{O}^{2-} = \text{CH}_3\text{COH}_{(\text{gas})} + \text{H}_2\text{O} + 2\text{e}^-$), so the equilibrium state is broken. The charge is transferred along with the current and the electric potential in the ITO becomes lower than before, so the electrons of the Sn metal will enter into the pyramid, as shown in Fig. 5b, and the resistance state of the whole device changes immediately. So the ultra sensitive detection is realized.

In conclusion, heavily Sn-doped In_2O_3 nano-pyramids have been obtained by meaning of using a sputtering approach. The gas sensors fabricated from these nano-pyramids are very sensitive to ethanol gas, demonstrating very fast response and recovery processes. The high response and the low working temperature have been achieved. These results demonstrate that heavily Sn-doped In_2O_3 nano-pyramids can be used as a gas sensing material for fabricating highly sensitive gas sensors.

The energy dispersive spectroscopy (EDS) spectra for nano-pyramids in different areas are used as [supplementary material-I](#). And the detailed calculation process of sensitivity is used as the [supplementary material-II](#).

This work was supported by the grant from the National Key R&D Program of China (NO. 2016YFB0400801), the Natural Science Foundation of Shaanxi Province (NO. 2017JQ6013) and the China Postdoctoral Science Foundation (NO. 2014M562415), and the Fundamental Research Funds for the Central Universities (NO. xjj2017011).

¹ X. Liu, S. Cheng, H. Liu, S. Hu, D. Zhang, and H. Ning, *Sensors* **12**, 9635 (2012).

² J. Ma, H. Fan, H. Tian, X. Ren, C. Wang, S. Gao, and W. Wang, *Sens. Actuators B* **262**, 17 (2018).

³ M. Davydova, A. Laposá, J. Smarhak, A. Kromka, N. Neykova, J. Nahlik, J. Kroutil, J. Drahošoupil, and J. Voves, *Beilstein J. Nanotechnol.* **9**, 22 (2018).

⁴ H. Fu, C. Hou, F. Gu, D. Han, and Z. Wang, *Sens. Actuators B* **243**, 516 (2017).

⁵ V. N. Singh, B. R. Mehta, R. K. Joshi, F. E. Kruijs, and S. M. Shivaprasad, *Sens. Actuators B* **125**, 482 (2007).

⁶ H. Yang, S. Wang, and Y. Yang, *CrystEngComm* **14**, 1135 (2012).

⁷ J. Zhao, T. Yang, Y. Liu, Z. Wang, X. Li, Y. Sun, Y. Du, Y. Li, and G. Lu, *Sens. Actuators B* **191**, 806 (2014).

⁸ C. Zhao, B. Huang, E. Xie, J. Zhou, and Z. Zhang, *Sens. Actuators B* **207**, 313 (2015).

- ⁹ B. Huang, C. Zhao, M. Zhang, Z. Zhang, E. Xie, J. Zhou, and W. Han, *Appl. Surf. Sci.* **349**, 615 (2015).
- ¹⁰ J. Y. Zhou, J. L. Bai, H. Zhao, Z. Y. Yang, X. Y. Gu, B. Y. Huang, C. H. Zhao, L. Cairang, G. Z. Sun, Z. X. Zhang, X. J. Pan, and E. Q. Xie, *Sens. Actuators B* **265**, 273 (2018).
- ¹¹ Y. Al-Hadeethi, A. Umar, A. A. Ibrahim, S. H. Al-Heniti, R. Kumar, S. Baskoutas, and B. M. Raffah, *Ceram. Int.* **43**, 6765 (2017).
- ¹² N. G. Patel, P. D. Patel, and V. S. Vaishnav, *Sens. Actuators B* **96**, 180 (2003).
- ¹³ S. Xu and Y. Shi, *Sens. Actuators B* **143**, 71 (2009).
- ¹⁴ V. S. Vaishnav, S. G. Patel, and J. N. Panchal, *Sens. Actuators B* **206**, 381 (2015).
- ¹⁵ M. Afshar, E. M. Preiß, T. Sauerwald, M. Rodner, D. Feili, M. Straub, K. König, A. Schütze, and H. Seidel, *Sens. Actuators B* **215**, 525 (2015).
- ¹⁶ N. Pinna, G. Garnweitner, M. Antonietti, and M. Niederberger, *J. Am. Chem. Soc.* **15**, 5608 (2005).
- ¹⁷ C. Li, D. Zhang, S. Han, X. Liu, T. Tang, and C. Zhou, *Adv. Mater.* **2**, 143 (2003).
- ¹⁸ L. Gao, F. Ren, Z. Cheng, Y. Zhang, Q. Xiang, and J. Xu, *CrystEngComm* **17**, 3268 (2015).
- ¹⁹ H. Jia, Y. Zhang, X. Chen, J. Shu, X. Luo, Z. Zhang, and D. Yu, *Appl. Phys. Lett.* **82**, 4146 (2003).
- ²⁰ X. Y. Xue, Y. J. Chen, Y. G. Liu, S. L. Shi, Y. G. Wang, and T. H. Wang, *Appl. Phys. Lett.* **88**, 201907 (2006).
- ²¹ V. S. Vaishnav, P. D. Patel, and N. G. Patel, *Thin Solid Films* **490**, 94 (2005).